

## Computer Simulations of Multiple-Quantum NMR Experiments. II. Selective Excitation

W. S. WARREN,\* J. B. MURDOCH,† AND A. PINES

*Department of Chemistry and Materials and Molecular Research Division, Lawrence Berkeley  
Laboratory, University of California, Berkeley, California 94720*

Received February 1, 1984

The effects of selective multiple-quantum pulse sequences have previously been analyzed by coherent averaging theory. However, convergence of the Magnus expansion used for those calculations is questionable in the experimentally important region of long cycle times. Exact density matrix evolutions are calculated here to show when the coherent averaging calculations will be reliable. In addition, simple selective sequences which cannot be treated by coherent averaging theory are also analyzed. © 1984 Academic Press, Inc.

In a previous paper (1) (henceforth designated as I) the effects of simple pulse sequences for broadband excitation of multiple-quantum NMR coherences were explored in detail by computer calculations. One important but surprising (from a perturbation theory perspective) result is that high multiple-quantum transitions (which are simple to analyze for coupling constants (2-4), relaxation rates (5-10), and molecular symmetry (11)) tend to be stronger on average than low multiple-quantum transitions. Nonetheless, the intensity of any individual transition decreases rapidly as the number of coupled spins increases, and this has so far proven to be a fundamental limitation of this technique.

Pulse sequences which selectively excite only a few transitions can largely overcome this limitation by enhancing the signal in the selected transitions. Experiments with very long pulse sequences (thousands of pulses) have indeed shown signal enhancements (12), and average Hamiltonian (coherent averaging) theory has been extended to describe these sequences (13-15). But the average Hamiltonian expansion is in powers of the cycle time (16, 17), which is long for these complicated sequences. Convergence may therefore be questionable. In addition, some very simple selective sequences (which only require a few pulses and might therefore be useful in other types of spectroscopy) cannot be treated by this approach.

In this paper we calculate the exact density matrix evolution of multilevel systems under the influence of selective excitation sequences. We find conditions where highly compensated sequences are useful (and some where the compensation is actually harmful) and produce simple sequences for selective excitation in isotropic and anisotropic systems. We believe that our results (together with those contained

\* Present address: Department of Chemistry, Princeton University, Princeton, N.J. 08540.

† Present address: Technicare Corporation, 29100 Aurora Rd., Solon, Ohio 44139.

in I) provide an essentially complete description of the production of homonuclear multiple-quantum coherence.

#### DESIGN OF SELECTIVE SEQUENCES

A sequence which is zero-order  $nk$ -quantum selective can be produced from any cyclic sequence of pulses and delays, using a technique called phase cycling (12-15), illustrated in Fig. 1a. Assume that the cyclic sequence has a duration  $\Delta\tau_p$  (called a subcycle) and a propagator  $U_0 = \exp(-i\mathcal{H}_0\Delta\tau_p)$  where  $\mathcal{H}_0$  is the effective Hamiltonian (16, 17). At the end of the interval  $\Delta\tau_p$ , the sequence is repeated with all radiation phase-shifted by  $\phi = 2\pi/n$  about the  $z$  axis, giving a new effective Hamiltonian  $\mathcal{H}_\phi$  and propagator  $U_\phi$ .  $\mathcal{H}_\phi$  is related to  $\mathcal{H}_0$  by a rotation of  $-\phi$  about the  $z$  axis:

$$\mathcal{H}_\phi = \exp(i\phi I_z)\mathcal{H}_0 \exp(-i\phi I_z), \quad [1]$$

$$(\mathcal{H}_\phi)_{ij} = (\mathcal{H}_0)_{ij} \exp(i\phi(M_i - M_j)), \quad [2]$$

and  $U_\phi$  is related to  $U_0$  in exactly the same manner. This phase shift is repeated  $n$  times, creating a cycle with cycle time  $t_c = n\Delta\tau_p$ . To lowest order the effective Hamiltonian for the full cycle is

$$\bar{\mathcal{H}}^{(0)} = \frac{1}{n} \sum_{l=0}^{n-1} \bar{\mathcal{H}}_{\phi^l}^{(0)} = \frac{1}{n} \sum_{l=0}^{n-1} \exp(il\phi I_z) \bar{\mathcal{H}}_0^{(0)} \exp(-il\phi I_z). \quad [3]$$

This sum scales the matrix element  $(\bar{\mathcal{H}}_0^{(0)})_{ij}$  by  $(1/n) \sum_{l=0}^{n-1} e^{i2\pi pl/n}$ , where  $p = m_i - m_j$ ; this scaling factor is zero unless  $p = nk$ . Therefore,  $\bar{\mathcal{H}}^{(0)}$  is a pure  $nk$ -

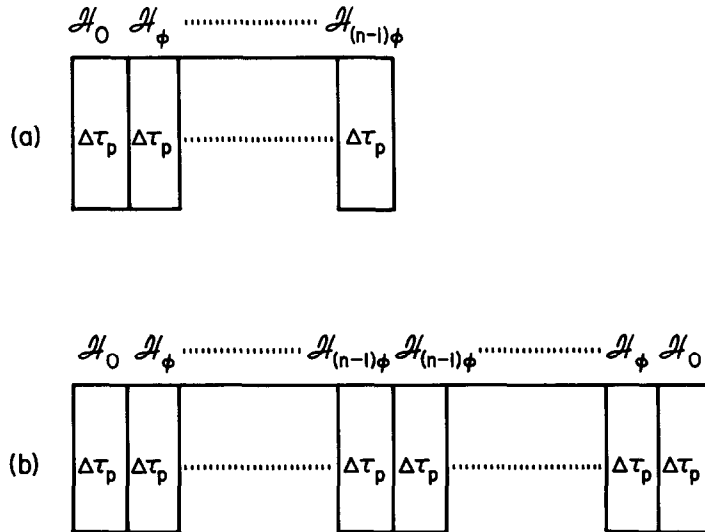


FIG. 1. (a) Phase cycling can be used to create  $nk$ -quantum selective sequences, using phase shifts of  $\phi = 2\pi/n$ . The cycle of  $n$  subcycles is more selective by one order in the average Hamiltonian theory expansion. (b) The cycle of  $2n$  subcycles formed by phase cycling and symmetrization is more selective by two orders. Reproduced, by permission of the publisher, from Ref. (15).

quantum selective operator, and  $U$  will only induce transitions between states with  $\Delta M = nk$  to first order in  $\Delta\tau_p$ .

It can also be shown that if  $\mathcal{H}_0$  is already  $j$ -order selective, then the sequence of Fig. 1a is  $(j + 1)$ -order selective (14, 15). Symmetrizing the sequence, as in Fig. 1b, can be shown to make all odd-order correction terms ( $\bar{\mathcal{H}}^{(2q+1)}$ , where  $q$  is any integer) vanish, permitting one to build a sequence with a specific level of selectivity from fewer subcycles than would be required from phase cycling alone. For example, a third-order  $nk$ -quantum selective sequence can be created by two phase cycles and two symmetrizations, for a total of  $4n^2$  subcycles; such a sequence is selective up to fourth order in  $\Delta\tau_p$ , and is illustrated for the case  $n = 4$  in Fig. 2.

The most important strength of this coherent averaging approach is its generality. For example, the pulse sequence represented schematically by Fig. 1a is zero-order  $nk$ -quantum selective, no matter what the Hamiltonian is, and no matter what the exact pulse sequence is for each subcycle. In addition, residual nonselective terms can be estimated for nonideal sequences, and this estimation only requires knowledge of the norm of the dipolar Hamiltonian  $\|\mathcal{H}_D\|$  and the fraction of  $nk$ -quantum operators in the subcycle effective Hamiltonian (15). In practice this generality is extremely useful, because the most interesting applications of selective excitation are to molecules with unknown dipolar couplings and chemical shifts. Even if the individual couplings are unknown,  $\|\mathcal{H}_D\|$  can be readily estimated from the width of the single-quantum spectrum; and if  $\|\mathcal{H}_D\Delta\tau_p\| \geq 1$ , the fraction of  $nk$ -quantum operators can be approximately calculated from the results in our previous paper (I).

However, this generality implies several important disadvantages. Even an infinite-order  $nk$ -quantum selective sequence (which would require an infinite number of

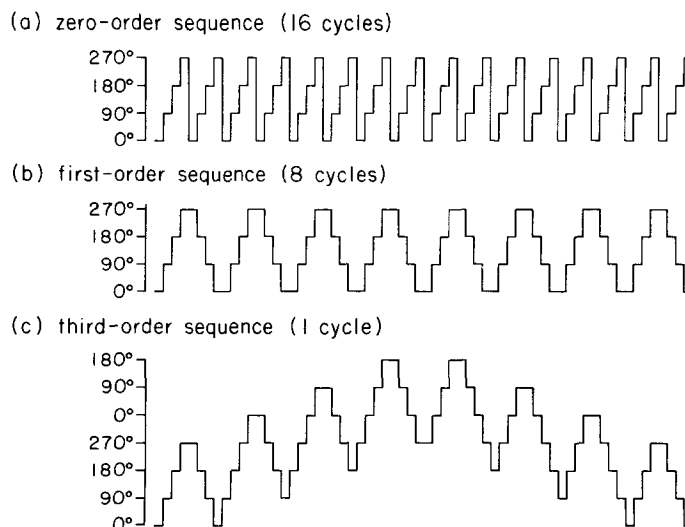


FIG. 2. A schematic comparison of the phases in different orders of pulse sequences for  $4k$ -quantum selection. For short cycle times higher order sequences are superior. For long cycle times they are not (see text).

pulses!) need not produce any  $nk$ -quantum coherences; after all, the null operator is by definition  $nk$ -quantum selective, because it cannot produce non- $nk$ -quantum coherences. A lower limit must be imposed on the cycle time if high-quantum operators are desired (15). Even if this requirement is met, an unfortunate choice of pulse sequence parameters might produce a subcycle effective Hamiltonian  $\mathcal{H}_0$  with a vanishingly small fraction of  $nk$ -quantum operators.  $\mathcal{H}_0$  cannot be calculated without prior knowledge of the coupling constants, no matter what the exact sequence is, because bilinear dipolar or  $J$  couplings are required to generate multiple-quantum coherences. Therefore, appropriate lengths for delays can only be estimated, not calculated exactly.

In addition, any calculation involving coherent averaging theory must be treated with caution unless convergence of the Magnus expansion can be shown. When convergence is questionable, the results can be completely wrong. As an example, consider the two sequences illustrated schematically in Fig. 3. Figure 3a is a zero-order  $2k$ -quantum selective sequence repeated twice; the second sequence is first-order  $2k$ -quantum selective, and consists of two phase cycles (or one phase cycle and symmetrization). The effective Hamiltonian for the first two subcycles can be written as  $\mathcal{H}_e + \epsilon\mathcal{H}_o$ , where  $\mathcal{H}_e$  is  $2k$ -quantum selective and  $\mathcal{H}_o$  is non- $2k$ -quantum selective (i.e., contains only odd-quantum operators) and  $\epsilon \ll 1$  is assumed. The exact propagator for the first sequence is then  $\{\exp[-i(\mathcal{H}_e + \epsilon\mathcal{H}_o)(2\Delta\tau_p)]\}^2$ . The effective Hamiltonian for the third and fourth subcycles of the second sequence is  $\mathcal{H}_e - \epsilon\mathcal{H}_o$ , since this half of the sequence is related to the first half by a phase shift of  $\pi$ ; therefore the exact propagator for the second sequence is

$$\exp(-i(\mathcal{H}_e + \epsilon\mathcal{H}_o)2\Delta\tau_p) \exp(-i(\mathcal{H}_e - \epsilon\mathcal{H}_o)2\Delta\tau_p). \quad [4]$$

Intuitively, one might expect the second sequence to always be superior to the first, since it is selective to higher order in the average Hamiltonian expansion. Equivalently, expansion of the exponentials in powers of  $\Delta\tau_p$  gives  $U = 1 - i(4\Delta\tau_p)(\mathcal{H}_e + \epsilon\mathcal{H}_o) + O(\Delta\tau_p^2)$  for the first sequence, and  $U = 1 - i(4\Delta\tau_p)(\mathcal{H}_e) + O(\Delta\tau_p^2)$  for the second sequence. However, when  $\|\mathcal{H}_e\Delta\tau_p\|$  is large, expansion in powers of  $\Delta\tau_p$  is invalid. As long as  $\epsilon \ll 1$ , a different expansion can be used (18):

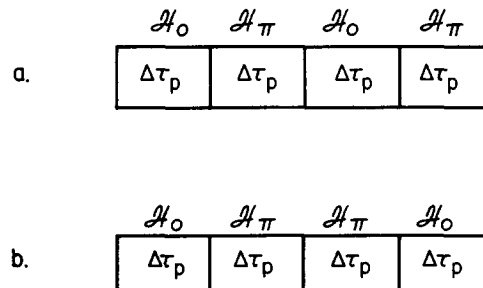


FIG. 3. Two pulse sequences which illustrate that average Hamiltonian theory must be used with caution. Part (b) is first-order  $2k$ -quantum selective, and part (a) is zero-order  $2k$ -quantum selective. The sequence in part (b) is more selective if  $\Delta\tau_p$  is small. The sequence in part (a) is more selective if  $\Delta\tau_p$  is large (see text).

$$\exp(A + \epsilon B)_{jk} = (\exp(A))_{jj} \delta_{jk} + \epsilon B_{jk} \left( \frac{\exp(A)_{jj} - \exp(A)_{kk}}{A_{jj} - A_{kk}} \right) + O(\epsilon^2). \quad [5]$$

$A$  and  $B$  are both written in a basis where  $A$  is diagonal, and  $B$  is assumed to be completely off-diagonal. Using this expansion one finds

$$\begin{aligned} \{[\exp(-i(\mathcal{H}_e + \epsilon \mathcal{H}_s)(2\Delta\tau_p))]\}_{jk}^2 &\approx \exp(-i\mathcal{H}_e 4\Delta\tau_p)_{jj} \delta_{jk} \\ &+ \epsilon(\mathcal{H}_s)_{jk} \left( \frac{\{\exp(-i\mathcal{H}_e(4\Delta\tau_p))_{jj} - \exp(-i\mathcal{H}_e(4\Delta\tau_p))_{kk}\}}{(\mathcal{H}_e)_{jj} - (\mathcal{H}_e)_{kk}} \right), \quad [6] \end{aligned}$$

$$\begin{aligned} \{\exp[-i(\mathcal{H}_e + \epsilon \mathcal{H}_s)(2\Delta\tau_p)] \exp[-i(\mathcal{H}_e - \epsilon \mathcal{H}_s)(2\Delta\tau_p)]\}_{jk} &\approx \exp(-i\mathcal{H}_e 4\Delta\tau_p)_{jj} \delta_{jk} \\ &- \epsilon(\mathcal{H}_s)_{jk} \left( \frac{\{\exp(-i\mathcal{H}_e(2\Delta\tau_p))_{jj} - \exp(-i\mathcal{H}_e(2\Delta\tau_p))_{kk}\}^2}{(\mathcal{H}_e)_{jj} - (\mathcal{H}_e)_{kk}} \right). \quad [7] \end{aligned}$$

As expected, the first nonselective term in Eq. [6] is proportional to  $\Delta\tau_p$  and the first nonselective term in Eq. [7] is proportional to  $(\Delta\tau_p)^2$ , so when  $\Delta\tau_p$  is small the first-order sequence is superior. When  $\Delta\tau_p$  is large, however,  $\exp(-i\mathcal{H}_e(2\Delta\tau_p))_{jj}$  and  $\exp(-i\mathcal{H}_e(4\Delta\tau_p))_{jj}$  are essentially random numbers of magnitude 1; thus, the root-mean-squared value of the term in brackets is  $\sqrt{2}$  in Eq. [6] and 2 in Eq. [7]. Therefore the first-order sequence is expected to actually be *worse* than the zero-order sequence for large  $\Delta\tau_p$ , where the average Hamiltonian calculation does not converge. This problem is by no means unique to selective excitation calculations. Any pulse sequence which attempts to retain a large term  $\mathcal{H}_L$  in the Hamiltonian while suppressing a smaller off-diagonal term  $\mathcal{H}_S$  (for example, a train of echo pulses to suppress chemical shifts and magnet inhomogeneity (19) in the presence of dipolar couplings) will require  $\|\mathcal{H}_L t_c\| \ll 1$ , not the weaker condition  $\|\mathcal{H}_S t_c\| \ll 1$ , as shown by this expansion.

It is useful to confirm selectivity calculations by a technique independent of average Hamiltonian theory, because of this convergence problem. For a small enough spin system with a given Hamiltonian, the exact effect of any pulse sequence can be calculated by solving the density matrix equation of motion on a computer. Since no approximations are required, such a calculation allows rigorous testing of the important concepts of the theory of selectivity, and in addition can show where convergence actually begins to be questionable. For this reason, computer studies were initiated. The results generally verify the calculations of Ref. (15) but give additional insight into the design of practical experimental sequences.

#### PROGRAMMING DETAILS

The propagator for any pulse sequence can be calculated by multiplying together the propagators for each individual pulse or delay. In a system with  $N$  spins  $1/2$ , each propagator can be written as a  $2^N \times 2^N$  matrix. Multiplying together two matrices of this size requires  $2^{3N}$  individual multiplications, so the number of matrix multiplications should be kept to a minimum. One way to do this is to use the simple relationship [1] between the propagators for different subcycles. Thus, once the propagator  $U_0$  for the first subcycle has been calculated, the propagator for any other phase-shifted subcycle can be calculated with  $2^{2N}$  multiplications, no matter

how many pulses the subcycle contains. Similarly, calculations for high-order sequences involving several phase cycles can be simplified by calculating the propagator after the first phase cycle, then using Eq. [1] on it.

$U_0$  can only be calculated exactly if  $\mathcal{H}$  is given. For some of the calculations, dipolar coupling constants, chemical shifts, and  $J$  couplings are explicitly specified in  $\mathcal{H}_D$ ,  $\mathcal{H}_{CS}$ , and  $\mathcal{H}_J$ . In other calculations the generality of the average Hamiltonian approach is retained by assuming a form for  $\mathcal{H}_0$ , usually one that has random matrix elements of roughly equal magnitude everywhere, subject only to the constraint that the matrix be Hermitian.

All computing was done on a VAX 11/780 system with a 2.5 Mbyte memory and floating point accelerator hardware. Several different random four-spin and five-spin systems were studied. Calculations for a third-order  $4k$ -quantum selective sequence on an unsymmetrical four-spin system with 125 different values for the cycle time required roughly 30 min of processor time; an unsymmetrical five-spin system required roughly four hours.

#### ZERO-ORDER SELECTIVE SEQUENCES

Figure 4 shows the effects of a zero-order  $4k$ -quantum selective sequence (Fig. 1a) on a four-spin system, starting with a random  $\mathcal{H}_0$  and  $U_0$ . The results from five random  $\mathcal{H}_0$  operators were averaged together. The triangles show, as a function of the cycle time, the ratio of a typical  $4k$ -quantum selective to a typical non- $4k$ -quantum selective matrix element of the propagator (the propagator selectivity  $S_p$ ). The propagator selectivity is proportional to  $(t_c)^{-1}$  for small  $t_c$ , which implies that the sequence does in fact have a nonselective ( $\mathcal{H}^{(1)}$ ). When  $t_c$  is large, the propagator selectivity is essentially unity.

$(\tilde{\mathcal{H}}^{(1)})_{\text{nns}}$  can be estimated using Theorem II of Ref. (15)

$$(\tilde{\mathcal{H}}^{(1)})_{\text{nns}} = \left( -\frac{1}{t_c} \int_0^{t_c} dt_2 \int_0^{t_2} dt_1 \mathcal{H}_{\phi(t_2)} \mathcal{H}_{\phi(t_1)} \right)_{\text{nns}} \quad [8]$$

where nns designates the non- $nk$ -quantum selective part. Since there are only four subintervals, there are only 10 terms  $\mathcal{H}_{\phi(t_2)} \mathcal{H}_{\phi(t_1)}$ , and the sum of terms with  $\phi(t_2) = \phi(t_1)$  is  $4k$ -quantum selective. If matrix elements for the remaining 6 terms add randomly

$$\|\tilde{\mathcal{H}}^{(1)} t_c\|_{\text{nns}} \sim \sqrt{6} \langle \|\mathcal{H}_{\phi(t_2)} \mathcal{H}_{\phi(t_1)} \Delta \tau_p^2\| \rangle_{\text{nns}} \sim \frac{\sqrt{6}}{16} \|\mathcal{H}_0 t_c\|^2 \quad [9]$$

where the norm of the  $n$  by  $n$  matrix  $\|A\|$  is defined as  $(\text{Tr}(A^2)/n)^{1/2}$ .

Of the 256 matrix elements, 72 are either populations, zero-quantum coherences, or four-quantum coherences, so that

$$\|\tilde{\mathcal{H}}^{(0)}\| \sim (72/256)^{1/2} \|\mathcal{H}_0\|, \quad [10]$$

$$S_p = \left( \frac{256 - 72}{72} \right)^{1/2} \|\tilde{\mathcal{H}}^{(0)} t_c\| / \|\tilde{\mathcal{H}}^{(1)} t_c\|$$

$$= 5.6 \|\mathcal{H}_0 t_c\|^{-1}. \quad [11]$$

Figure 4 gives  $S_p = 7.8 \|\mathcal{H}_0 t_c\|^{-1}$ ; the agreement is good, as expected since short cycle times should give rapid convergence.

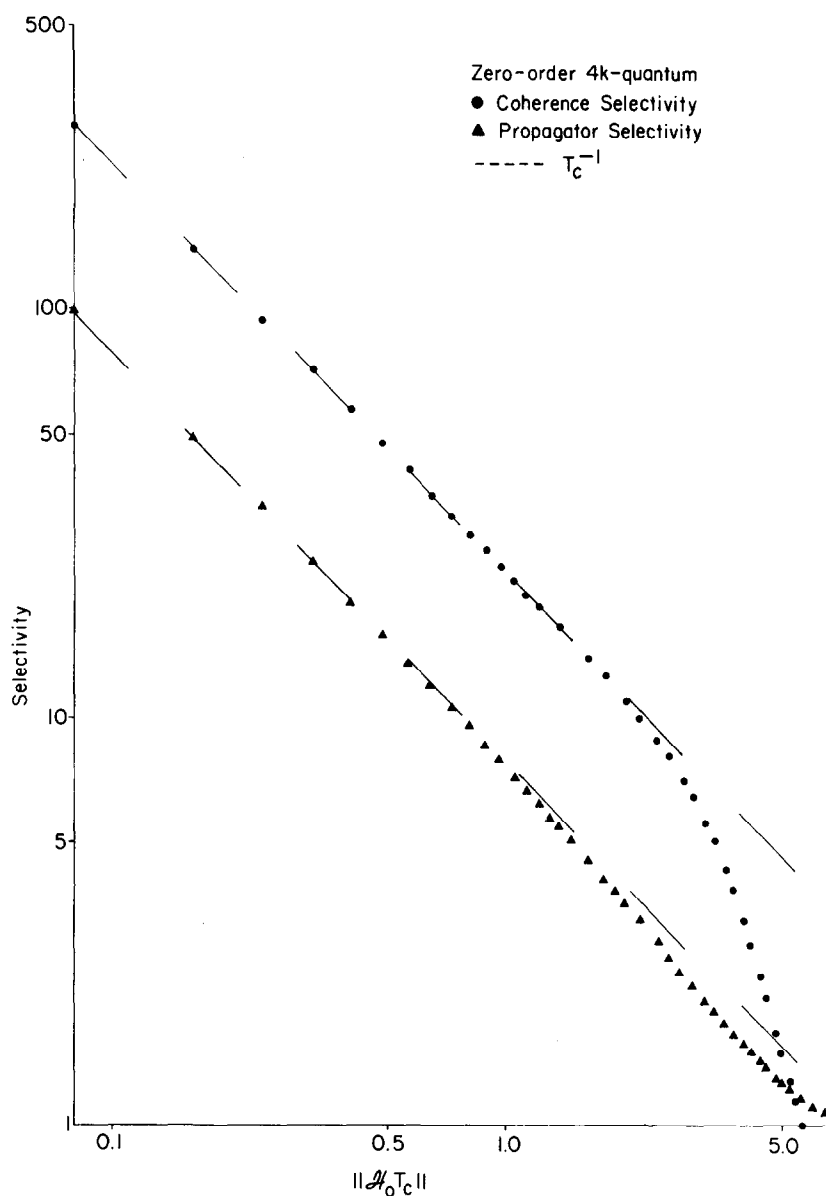


FIG. 4. The propagator selectivity and coherence selectivity of one cycle of a zero-order  $4k$ -quantum selective sequence. Both selectivities are proportional to  $T_c^{-1}$  for short cycle times, which indicates that  $\hat{\mathcal{H}}^{(1)}$  does not vanish.

Figure 4 also shows the ratio of the magnitude of a typical four-quantum coherence in the final density matrix to the magnitude of a typical one-, two-, or three-quantum coherence, as a function of the cycle time. This ratio will be called the coherence selectivity. The coherence selectivity is experimentally observable if the signal-to-noise ratio is sufficiently good, so it is more useful than the propagator selectivity. However, it cannot be readily calculated from coherent averaging theory.

Even if the effective Hamiltonian  $\tilde{\mathcal{H}}$  is completely known, the coherence selectivity requires calculation of  $\exp(-i\tilde{\mathcal{H}}t_c)I_z \exp(i\tilde{\mathcal{H}}t_c)$ , which is difficult to evaluate by hand for any reasonably sized system unless  $\|\tilde{\mathcal{H}}t_c\|$  is small.

Fortunately, the coherence selectivity is usually larger than the selectivity of the effective Hamiltonian. This can be readily seen by expanding  $\rho$  in powers of  $t_c$ :

$$\rho = I_z - it_c[\tilde{\mathcal{H}}, I_z] + O(t_c^2), \quad [12]$$

$$[\tilde{\mathcal{H}}, I_z]_{jk} = (\tilde{\mathcal{H}})_{jk}(M_j - M_k). \quad [13]$$

$M_j - M_k$  is larger for the four-quantum transition than for any other transition, so the coherence selectivity is strengthened in the lowest order term. In fact, since there are 8 three-quantum transitions, 28 two-quantum transitions, and 56 one-quantum transitions,  $\langle \Delta M \rangle_{\text{nns}} = 1.48$ , and the 4Q coherence selectivity should be roughly 2.7 times larger than the effective Hamiltonian selectivity on the average. (In Fig. 3 the ratio for small  $t_c$  is 2.95, but this value depends on the choice of matrix elements for  $U_0$ .) Thus, since the selectivity from coherent averaging theory provides an underestimate for the coherence selectivity, it is still a useful test for convergence.

#### SIGNAL INTENSITIES

Figure 5 shows the observable signal intensity for the four-quantum transition (the square of the coherence magnitude, as noted in I) as a function of the cycle time, in units of  $\beta = (2)^{-N}(\hbar\omega_0/kT)$ . The total available signal  $\beta \text{Tr}(I_z^2) = 16\beta$ , and there are 256 matrix elements, so the expectation value (from a statistical model) of the signal from nonselective excitation is  $0.0625\beta$ . As shown in I, an exact calculation would give between 2 and 6.5 times more signal. The theoretical maximum is  $4.00\beta$ , corresponding to a complete transfer of the largest equilibrium population difference into this single coherence (15). The largest signal from Fig. 5a, however, is 2.22 when  $\|\tilde{\mathcal{H}}^{(0)}t_c\| = 2.1$ . At the peak, the computed propagator selectivity is only 3.40; the comparatively large values of  $t_c$  required to pump four-quantum operators make the selectivity disappear before the true maximum can be reached. This is not surprising; since the first maximum corresponds to a selective  $90^\circ$  pulse between the two extreme levels, the coefficient of the four-quantum operator in  $\tilde{\mathcal{H}}^{(0)}$  must be at least  $\pi/4$ . We then expect  $\|\tilde{\mathcal{H}}^{(0)}t_c\| \geq (\pi/4)(72/16)^{1/2} = 1.67$  if all 72  $4k$ -quantum operators are pumped equally, and  $\|\mathcal{H}_0t_c\| \sim 3.14$ . This is well outside of the range of convergence; in fact, the computed propagator selectivity is only 1.74 for this cycle time.

Several approaches can be taken to improve the selectivity. The first, and simplest, is to decrease the cycle time and increase the number of cycles. For convenience define  $T_c$  as the number of cycles times the cycle time;  $T_c$  is then the total duration. If two cycles are used, for example,  $\|\mathcal{H}_0T_c\| \sim 3.14$  for the whole sequence when  $\|\mathcal{H}_0t_c\| \sim 1.57$  for each cycle. Thus larger signals should be attainable, as illustrated in Fig. 5b; the maximum is now 3.19 at  $\|\mathcal{H}_0T_c\| = 2.75$ .

The signal can be further increased by adding more cycles. With 16 cycles, the signal follows a  $\sin^2$  curve for several oscillations, as shown in Fig. 6. The maximum gain is achieved when  $\|\mathcal{H}_0T_c\| = 3.2$ , with a signal of  $4.00\beta$ . This  $\sin^2$  pattern is expected, since the four-quantum sequence creates an effective two-level system



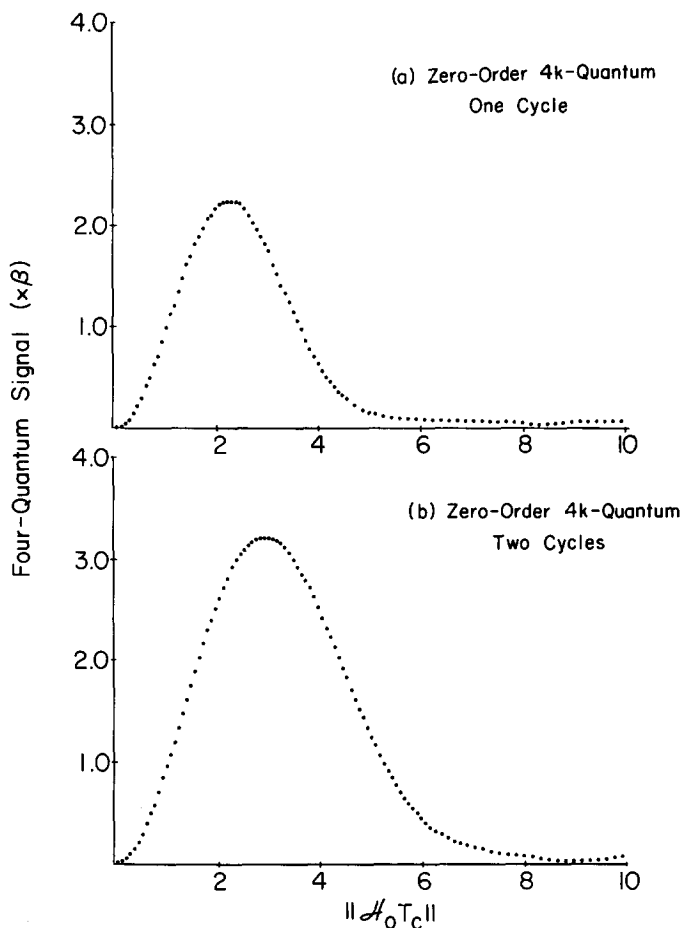


FIG. 5. (a) The signal produced by one cycle of a zero-order  $4k$ -quantum selective sequence as a function of the cycle time. The maximum attained signal is  $2.22\beta$ , which represents a gain of 36 relative to the statistical prediction for nonselective excitation. (b) The signal produced by two cycles of a zero-order  $4k$ -quantum selective sequence. The maximum attained signal is  $3.19\beta$ , which represents a gain of 51 relative to the statistical prediction for nonselective excitation.

between  $M = +2$  and  $M = -2$ . Thus  $\|\mathcal{H}_0 T_c\| = 3.2$  is a selective  $\pi/2$  pulse for this choice of  $\mathcal{H}_0$ ;  $\|\mathcal{H}_0 T_c\| = 6.4$  is a selective  $\pi$  pulse, which inverts the populations of the two extreme states. The oscillations die away as the selectivity disappears; if enough cycles are applied, however, they can be prolonged indefinitely.

The potential signal gain from lower-quantum selection is smaller (15) but still substantial. As an example, Fig. 7 shows the signal obtainable from  $5k$ -quantum selection or  $4k$ -quantum selection on a five-spin system. The five-quantum signal follows the normal  $\sin^2$  pattern of  $Nk$ -quantum selection in an  $N$ -spin system; the maximum signal is equal to the value of  $\beta I_z^2$  for the extreme states, which is  $6.25\beta$ ; and the gain is  $N2^N = 160$  relative to the statistical model (15). The maximum signal attained from four-quantum selection is  $0.80\beta$ , which corresponds to a gain of 20.5. The average signal from  $\|\mathcal{H}_0 T_c\| = 10$  to  $\|\mathcal{H}_0 T_c\| = 20$  is  $0.40\beta$ , for a gain of 10.3. The estimated gain from Ref. (15) for  $(N - 1)$ -quantum selection is 14.5.

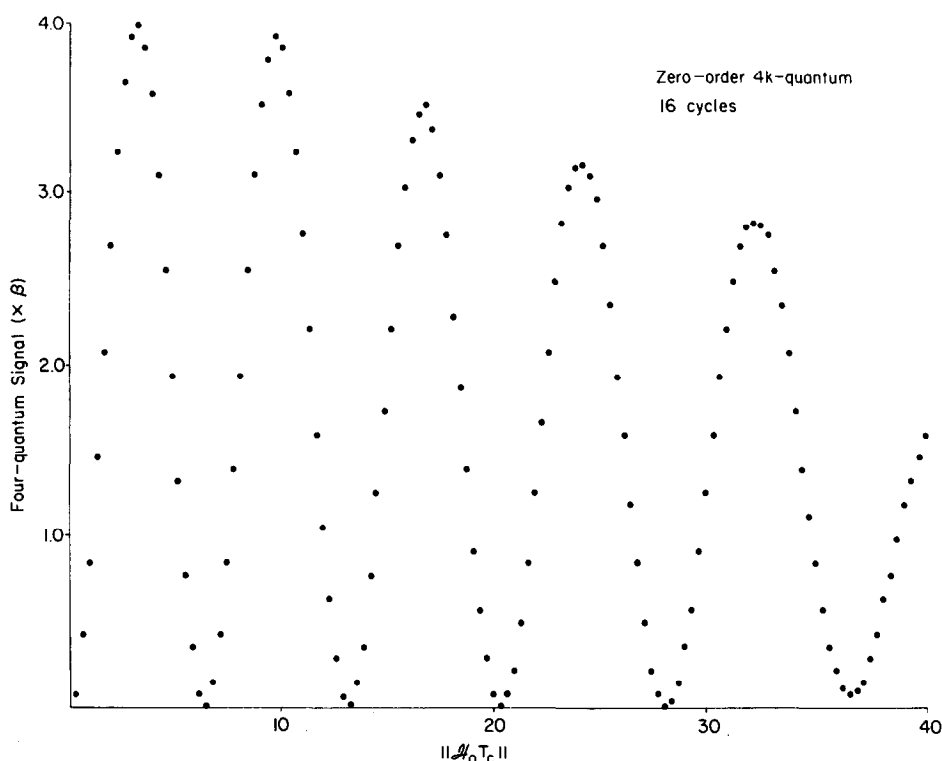


FIG. 6. The signal produced by 16 cycles of a zero-order  $4k$ -quantum selective sequence. The signal follows a  $\sin^2$  pattern for several oscillations, and reaches the theoretical maximum of  $4.00\beta$  for a gain of 64 relative to the statistical model for nonselective excitation.

#### HIGHER-ORDER SELECTIVE SEQUENCES

Another approach to improving selectivity is to use high-order selective sequences. Two different principles (nesting phase cycles and symmetrizing phase cycles) were used to design  $j$ -order  $nk$ -quantum selective sequences for arbitrary  $j$ ; if  $j$  is odd, such sequences require  $(2n)^{(j+1)/2}$  subcycles. Thus, the higher the order of selectivity, the longer the cycle time. This makes average Hamiltonian calculations much more complicated. For example, a third-order  $4k$ -quantum selective sequence has a cycle time 16 times longer than a zero-order  $4k$ -quantum sequence, so it is not obvious that  $\|\tilde{\mathcal{H}}^{(4)} t_c\|_{\text{nns}}$  for the former is always smaller than  $\|\tilde{\mathcal{H}}^{(1)} t_c\|_{\text{nns}}$  is for the latter. In fact, it was shown earlier that high-order selection is useless if  $t_c$  is large. If  $t_c$  is small, however, higher-order selection must be beneficial; in this example, the first nonselective operator in the propagator for the zero-order sequence is proportional to  $t_c^2$ , but the first nonselective operator for the third-order sequence is proportional to  $t_c^5$ . Thus an important question is how large  $t_c$  can be before high-order selection becomes useless.

Figure 8 compares the propagator selectivity of two cycles of zero-order  $4k$ -quantum selection with one cycle of first-order  $4k$ -quantum selection for a four-spin system. As expected the first-order sequence is far superior for short cycle times. At  $\|\mathcal{H}_0 T_c\| = 4.0$  the two curves cross, and for all later times the zero-order

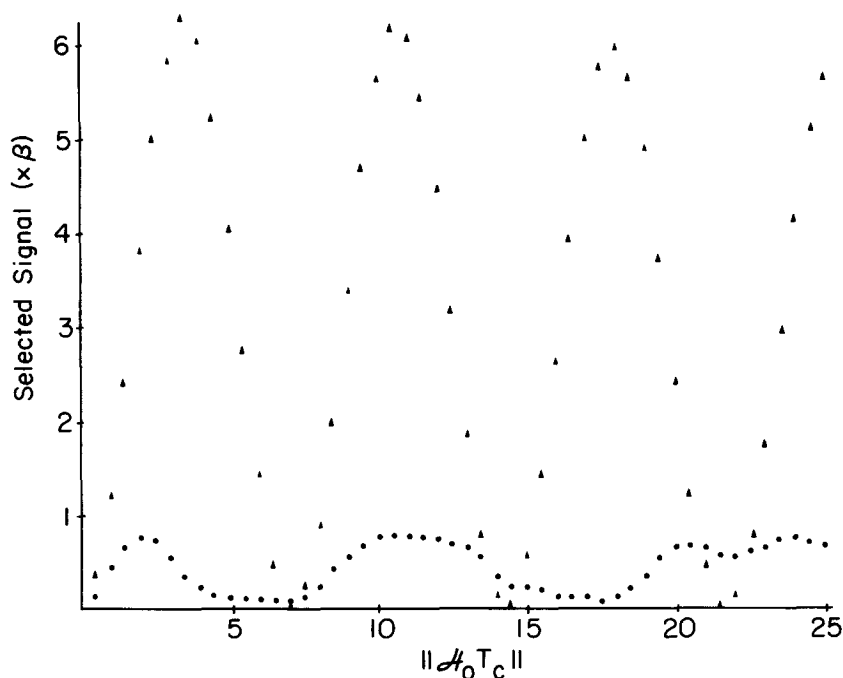


FIG. 7. The signal per transition produced by  $4k$ -quantum selection (circles) or  $5k$ -quantum selection (triangles) on a 5-spin system. The gain for  $5k$ -quantum selection is much larger than the gain for  $4k$ -quantum selection.

sequence is superior. However, the theoretical position of the first maximum (from Fig. 5) is smaller than this critical value, so the improved selectivity of the first-order sequence near that maximum produces a larger four-quantum signal ( $3.50\beta$  versus  $3.19\beta$  in Fig. 5b). For larger values of  $\|\mathcal{H}_0 T_c\|$  both the first-order and the repeated zero-order sequence have little selectivity, so the repeated zero-order sequence is never significantly superior. By contrast, Fig. 9 shows the signal from a third-order  $4k$ -quantum selective sequence. This should be compared with 16 cycles of a zero-order sequence, shown in Fig. 6. Again the high-order sequence is much more selective for short cycle times; the selectivities  $S_p$  are equal at 8.1 when  $\|\mathcal{H}_0 t_c\| = 14.7$ , and the zero-order sequence is superior after that. At the first maximum, the propagator selectivity of the third-order sequence is 1103 (Fig. 9), compared to only 44 for the zero-order sequence. However, both of these numbers are fairly large, so the signals are very nearly equal. (For larger spin systems the improved selectivity is much more important.) At the second maximum the selectivities are 21.3 and 12.0, and these numbers are small enough to make the third-order sequence somewhat better. At the third maximum the selectivities are almost equal. After the third maximum the selectivity of the third-order sequence dies away rapidly, but the repeated zero-order sequence remains partially selective for several oscillations.

Figure 10 shows the propagator selectivity of the third-order sequence, plotted on a log-log scale. For small values of  $t_c$  ( $\|\mathcal{H}_0 t_c\| \leq 5$ ) the selectivity is proportional to  $t_c^{-4}$  (the solid line in the figure) as expected when  $\tilde{\mathcal{H}}^{(4)}$  is the dominant nonselective

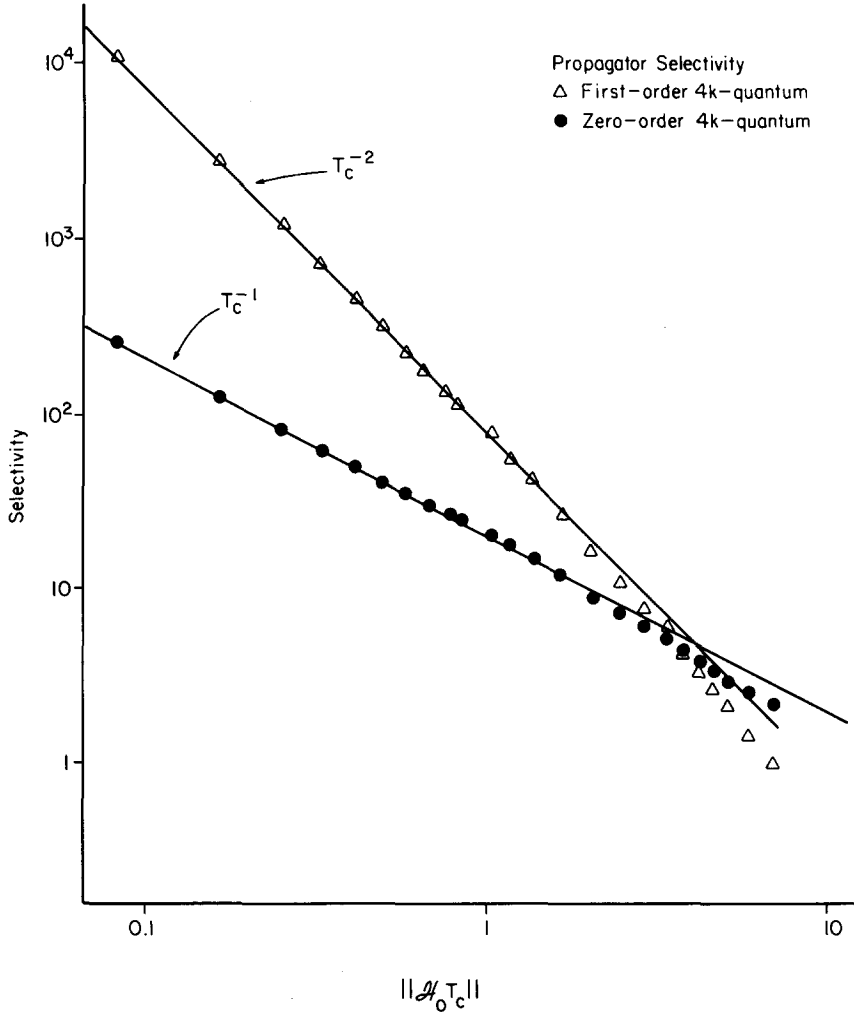


FIG. 8. The propagator selectivity of two cycles of zero-order  $4k$ -quantum selection, versus one cycle of first-order  $4k$ -quantum selection. The first-order selection is superior for short cycle times.

term and  $\tilde{\mathcal{H}}^{(0)}$  is the dominant  $4k$ -quantum selective term. The selectivity begins to deviate from the line around  $\|\mathcal{H}_0 t_c\| \sim 6$ . The initial deviation is in the favorable direction, which must reflect another selective term, presumably  $\tilde{\mathcal{H}}^{(2)}$ . In fact, the selectivity between  $\|\mathcal{H}_0 t_c\| = 10$  and  $\|\mathcal{H}_0 t_c\| = 20$  is proportional to  $t_c^{-2}$  (the dotted line in the figure), which would be expected if the dominant selective term were  $\tilde{\mathcal{H}}^{(2)}$ . For  $\|\mathcal{H}_0 t_c\| > 20$  the selectivity falls off rapidly, which probably indicates that  $\tilde{\mathcal{H}}^{(6)}$  and higher-order nonselective terms cannot be neglected.

A convergence criterion was derived in Ref. (15) by finding the value of the cycle time which would make the first  $n$ ns term from a  $j$ -order  $nk$ -quantum selective sequence (in this case,  $\|\tilde{\mathcal{H}}^{(4)}\|_{\text{nns}}$ ) equal to the first  $n$ ns term of a  $(j - 2)$ -order sequence repeated  $2n$  times. This intercept point was calculated to be  $\|\mathcal{H}_0 t_c\| \sim 6.8$  for  $4k$ -quantum selection. The propagator selectivity of eight repetitions of a first-order  $4k$ -quantum selective sequence intercepts the selectivity of this third-order

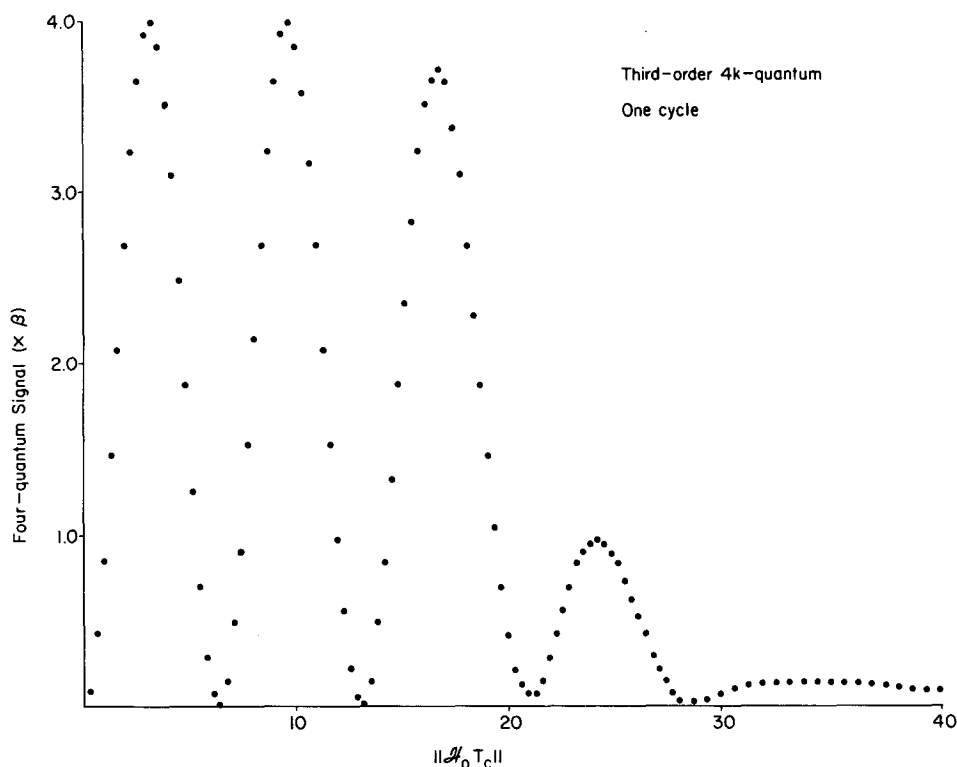


FIG. 9. The signal produced by one cycle of third-order  $4k$ -quantum selection. Comparison with Fig. 6 (16 cycles of zero-order selection) shows that the high-order sequence is somewhat superior for short cycle times but inferior for long cycle times.

sequence at  $\|\mathcal{H}_{0t_c}\| = 5.1$ . The agreement is good, particularly since the convergence criterion is merely an estimate based on random addition of nonselective terms (similar to Eq. [9]) and a four-spin system is fairly small for such an assumption. In fact, this convergence criterion is a conservative estimate; the selectivity is still around 100 when  $\|\mathcal{H}_{0t_c}\| = 6.8$ .

High-order selective sequences are of course also useful for  $(N - 1)$ -quantum and lower-quantum transitions. In fact, the calculation of the selectivity in Ref. (15) does not depend on the number of spins in the system. Computer calculations verify that the number of spins is not important. For example, the propagator selectivity of a third-order  $4k$ -quantum selective sequence on benzene deviates by less than 10% from the selectivity in Fig. 10 throughout the region of convergence  $\|\mathcal{H}_{0t_c}\| \leq 5$ . The signal from a third-order  $4k$ -quantum sequence on a five-spin system is identical to the signal from 16 zero-order  $4k$ -quantum sequences (shown in Fig. 7) through the first maximum; is slightly larger on average through  $\|\mathcal{H}_{0T_c}\| \sim 12.8$ , where the propagator selectivities of both sequences are equal; and is smaller on average for larger values of  $T_c$ .

Thus, high-order selective sequences can increase the signal in the selective experiment. They are expected to become even more important for larger systems, where the required selectivity for maximum signal is greater. Since the agreement between average Hamiltonian theory and exact calculations is extremely good for

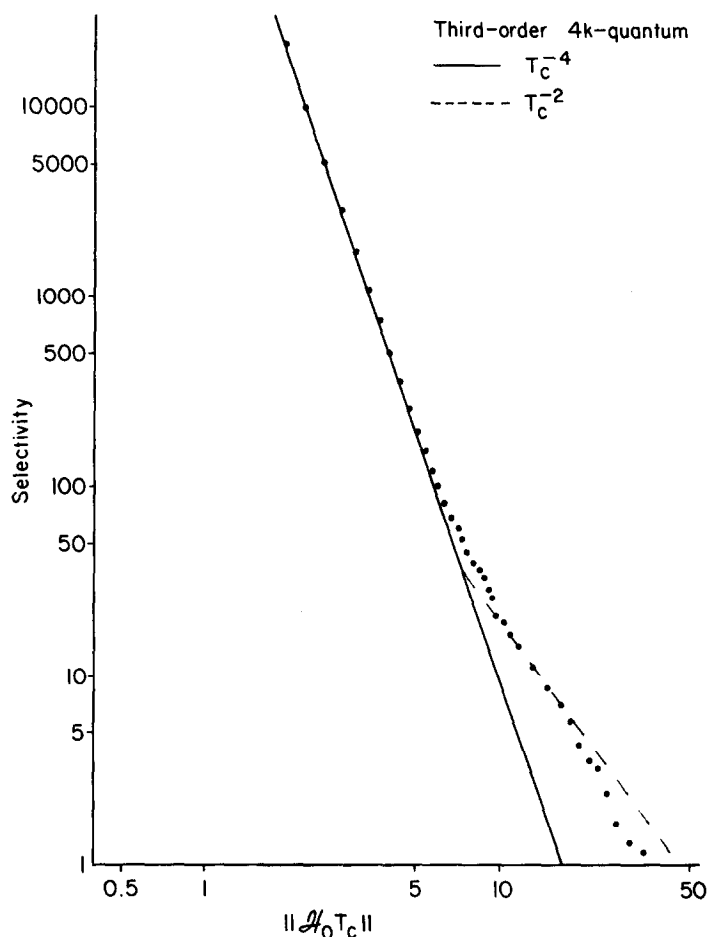


FIG. 10. The propagator selectivity of a third-order  $4k$ -quantum selective sequence. The selectivity is proportional to  $T_c^{-4}$  for short values of the cycle time. Deviations from this line occur in the region predicted by the convergence criteria of Ref. (15).

the systems in this section, it is very likely that the average Hamiltonian calculations are valid for larger systems that cannot be exactly analyzed.

#### EXACT CALCULATIONS FOR SIMPLE SEQUENCES

In all of the computer calculations discussed so far, the exact form of  $\mathcal{H}_0$  was assumed, not calculated. Thus, some unspecified pulse sequence creates multiple-quantum coherences with a propagator  $U_0$  and effective Hamiltonian  $\mathcal{H}_0$ , and these two operators contain equal amounts of multiple-quantum operators corresponding to all values of  $\Delta M$ . The experiments in Ref. (12) were done with time-reversing sequences (20). For such sequences equal intensities would be the best guess for  $\mathcal{H}_0$ . However, time-reversal sequences involve thousands of pulses, and this generally implies problems with sample heating and stability of the pulse trains. In addition, there are important applications in which perfect time reversal is not even theoretically possible, such as in isotropic systems.

In this section, the assumption of time reversal will be discarded. Specific pulse sequences will be applied to systems with known Hamiltonians. These Hamiltonians sometimes correspond to specific molecules, and sometimes are random. These calculations show that time reversal, while useful, is not essential to the design of selective sequences.

The simplest possible cyclic pulse sequence for  $\mathcal{H}_0$  would be two pulses with a delay between them. If the pulses are assumed to have phase  $\gamma$  and  $\bar{\gamma}$  and flip angle  $\pi/2$ , then  $\mathcal{H}_0 = \mathcal{H}_x$ , where  $\mathcal{H}_x$  is the operator which generates multiple-quantum coherences in the nonselective experiment and was analyzed in I. It only has 0-quantum, 1-quantum, and 2-quantum operators; in the nonselective experiment high-quantum operators are generated by the complex exponential in the propagator. However, higher-quantum operators must be present in  $\mathcal{H}_0$  if zero-order selection is to work. Thus, a zero-order  $4k$ -quantum selective sequence is not expected to produce much four-quantum signal.

The general form of  $\tilde{\mathcal{H}}^{(j)}$  can be calculated readily from coherent averaging theory. Since all operators in  $\mathcal{H}_x$  are at most bilinear,  $\tilde{\mathcal{H}}^{(1)}$  involves at most three spins, and cannot have four-quantum operators.  $\tilde{\mathcal{H}}^{(2)}$  can have four-quantum operators, so a second-order or third-order  $4k$ -quantum selective sequence might be useful. Unfortunately, short cycle times imply a small  $\tilde{\mathcal{H}}^{(2)}$ , and  $\tilde{\mathcal{H}}^{(0)}$  does not vanish. If the cycle time becomes long enough to make  $\|\tilde{\mathcal{H}}^{(2)}T_c\| \sim 1$ , then  $\|\tilde{\mathcal{H}}^{(0)}T_c\| \gg 1$  and the Magnus expansion does not converge. As a result, even high-order selective sequences are not expected to provide much signal enhancement with this form for  $\mathcal{H}_0$ , as was confirmed by computer calculations.

The convergence problem can be solved by using a line-narrowing sequence for  $\mathcal{H}_0$  (15, 21) (i.e., a sequence whose zero-order average Hamiltonian  $\tilde{\mathcal{H}}^{(0)}$  is very small). For example, the WAHUA (16) sequence ( $T-90_x-T-90_y-2T-90_{\bar{y}}-T-90_x-T$ ) gives  $\tilde{\mathcal{H}}^{(0)} = \tilde{\mathcal{H}}^{(1)} = 0$  for all purely dipolar terms. Since the first useful term is then  $\tilde{\mathcal{H}}^{(2)}$  it is clear that the coherent averaging expansion will converge slowly, and then predictions based on computer calculations are more trustworthy.

Figure 11 shows the effect on the selectivity of varying  $T$  in a WAHUA sequence for  $\mathcal{H}_0$ . The sequence is incorporated into a zero-order  $4k$ -quantum selective sequence on a four-spin system. When  $T$  is small, the largest term in  $\mathcal{H}_0$  is  $\tilde{\mathcal{H}}_{cs}^{(0)} = (-1/3)(\sum \sigma_i(I_{xi} + I_{yi} + I_{zi}))$ ; zero-order selection suppresses the nonsecular part of this, but creates a non-selective  $\tilde{\mathcal{H}}^{(1)}$ . Thus, the coherence selectivity goes to 0 as  $\Delta\tau_p \rightarrow 0$ ; the propagator selectivity becomes very large because of the secular terms in  $\tilde{\mathcal{H}}^{(0)}$ , but these terms will not produce coherences. If  $T$  is small, the largest nns operator in  $\mathcal{H}_0$  is  $\tilde{\mathcal{H}}^{(1)}$ , proportional to  $T$ ; the largest  $4k$ -quantum selective operator is  $\tilde{\mathcal{H}}^{(2)}$ , proportional to  $T^2$ , so the selectivity is proportional to  $T$ . Contrast this result with all the examples shown earlier in which the selectivities were proportional to negative powers of  $T_c$  and grew very large as  $T_c \rightarrow 0$ . As  $T$  is further increased,  $\tilde{\mathcal{H}}^{(3)}$  becomes the dominant nonselective term and the selectivity falls off as  $T^{-1}$ .

Figure 12 shows the signal produced by this sequence. When  $T$  is small, the signal is proportional to  $T^6$  because  $U \sim \exp(i\tilde{\mathcal{H}}^{(2)}T_c)$  produces coherences proportional to  $T^3$ . When  $\|\mathcal{H}_D T\| \sim 1$ , the selectivity is good and the signal is large; in fact, the maximum signal ( $2.98\beta$ ) is substantially larger than the maximum achieved by one cycle of  $4k$ -quantum selection using time reversal (Fig. 5a). Yet

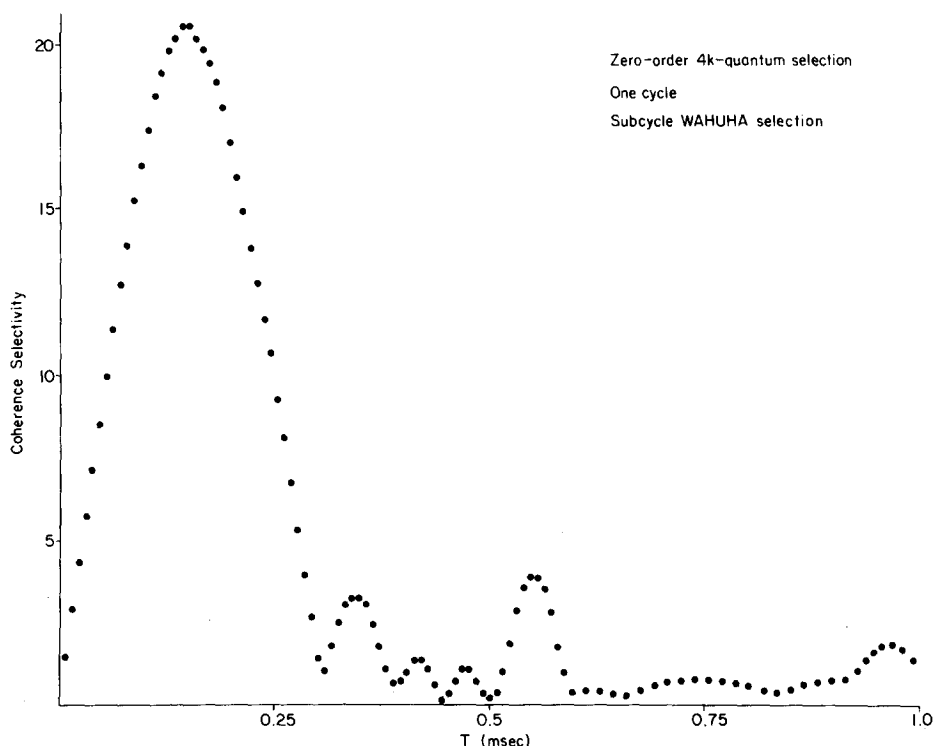


FIG. 11. The selectivity for one cycle of zero-order  $4k$ -quantum selection using a WAHUHA sequence for  $\mathcal{H}_0$ . The selectivity is proportional to  $T$  for short cycle times, because  $\tilde{\mathcal{H}}^{(1)}$  is nonselective and  $\tilde{\mathcal{H}}^{(2)}$  has  $4k$ -quantum operators. In the region of interest  $\|\tilde{\mathcal{H}}^{(2)}\| \gg \|\tilde{\mathcal{H}}^{(1)}\|, \|\tilde{\mathcal{H}}^{(3)}\|$ .

this sequence requires only 16 pulses, so sample heating and pulse instability are much less troublesome.

The maximum signal can be increased by using high-order selection or increasing the number of cycles. Figure 13 shows the effect of fixing  $T$  at  $120 \mu\text{s}$  and incrementing the number of cycles; the familiar  $\sin^2$  pattern appears. (In this four-spin simulation the average dipolar coupling is 400 Hz.) The period of the oscillations is proportional to  $T^3$ , since the dominant term in  $\mathcal{H}_0$  is  $\tilde{\mathcal{H}}_D^{(2)}$ . For this reason, the maximum may be hard to find in systems with unknown dipolar couplings.

Since  $\tilde{\mathcal{H}}_D^{(2)}$  has no operators with  $\Delta M > 4$ , high-quantum selection must rely on higher-order terms, and zero-order selection is ineffective. In such cases a different line-narrowing sequence may be helpful. A 12-pulse sequence which has  $\tilde{\mathcal{H}}_D^{(4)}$  as its leading dipolar term is  $(\tau-90_{\bar{x}}-\tau-90_{\bar{y}}-2\tau-90_{\bar{x}}-\tau-90_{\bar{y}}-2\tau-90_{\bar{x}}-\tau-90_{\bar{y}}-2\tau-90_{\bar{y}}-\tau-90_{\bar{x}}-2\tau-90_{\bar{y}}-\tau-90_{\bar{x}}-\tau)$ .

Computer calculations show that this sequence can be used for  $\mathcal{H}_0$  if  $6k$ -quantum selection is desired. It is most useful when the chemical-shift differences are small; if this is not the case then the simplest modification is to insert a  $180^\circ$  pulse in the middle of each delay. Each of these inserted pulses should be  $180^\circ$  out of phase with the  $90^\circ$  pulse which precedes it, to minimize rf inhomogeneity effects. Clearly,



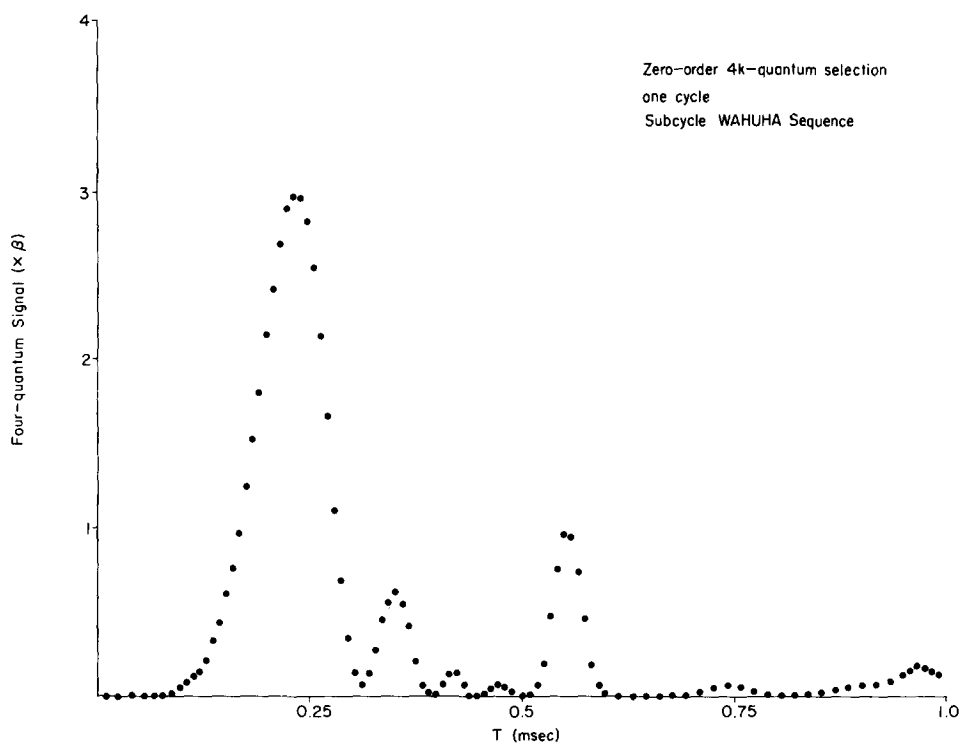


FIG. 12. The signal produced by one cycle of zero-order  $4k$ -quantum selection on a four-spin system, using a WAHUHA sequence for  $\mathcal{H}_0$ .

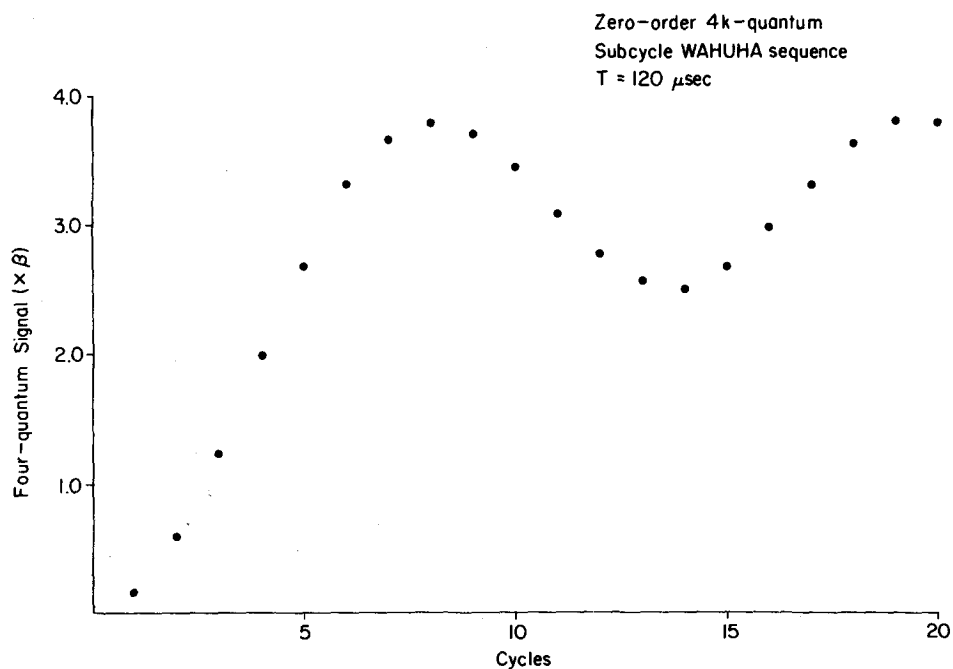


FIG. 13. The effect of fixing  $T$  at  $120 \mu\text{s}$  in a WAHUHA sequence for  $\mathcal{H}_0$  and incrementing the number of cycles of zero-order  $4k$ -quantum selection. Signal intensities that are as large as in the time-reversal experiment can be obtained.

the larger the number of quanta to be selected, the more complicated  $\mathcal{H}_0$  becomes, and this will be a practical limitation to the technique. Nonetheless, the advantage of very low duty cycles makes the use of line-narrowing sequences an attractive option for low-quantum selection.

#### SELECTIVITY IN ISOTROPIC SYSTEMS

For the reasons discussed in our previous paper I, multiple-quantum coherences are produced more slowly in isotropic systems than in anisotropic ones. In fact,  $\|\mathcal{H}_J \Delta \tau_p\| \sim 1$  will be required to give  $\mathcal{H}_0$  multiple-quantum coherences.  $\mathcal{H}_J$  cannot be time reversed by wideband pulses; however,  $\mathcal{H}_{cs}$  can be reversed, and since  $\|\mathcal{H}_{cs}\| \gg \|\mathcal{H}_J\|$  an appropriately chosen sequence will give selection. For example, consider the sequence in Fig. 14 where the first three pulses are the first subcycle. Let  $\mathcal{H}_x = -\sum \sigma_i I_{xi} + \sum_{i>j} J_{ij} \mathbf{I}_i \cdot \mathbf{I}_j$ , created by the sequence  $90_y - T - 90_{\bar{y}}$ ; and let  $\mathcal{H}_{-x} = \sum \sigma_i I_{xi} + \sum_{i>j} J_{ij} \mathbf{I}_i \cdot \mathbf{I}_j$  created by the sequence  $90_{\bar{y}} - T - 90_y$ . An average Hamiltonian expansion will not converge rapidly for  $\|\mathcal{H}_J T\| \sim 1$ , since then  $\|\mathcal{H}_{cs} T\| \gg 1$ . But the propagator can be expanded, using Eq. [5]:

$$\begin{aligned} U &= \exp(-i\mathcal{H}_x T) \exp(-i\mathcal{H}_{-x} T) \\ &= (\exp(-i(-\sum \sigma_i I_{xi} + \sum J_{ij} I_{xi} I_{xj}) T) + A)(\exp(-i(\sum \sigma_i I_{xi} + \sum J_{ij} I_{xi} I_{xj}) T) + B) \\ &= \exp(-2i \sum J_{ij} I_{xi} I_{xj} T) + A \exp(-i(\sum \sigma_i I_{xi} + \sum J_{ij} I_{xi} I_{xj}) T) \\ &\quad + \exp(-i(-\sum \sigma_i I_{xi} + \sum J_{ij} I_{xi} I_{xj}) T) B + AB, \quad [14] \end{aligned}$$

where

$$A_{kl} = (\sum J_{ij} (I_{zi} I_{zj} + I_{yi} I_{yj}))_{kl} \frac{\{\exp(-i(-\sum \sigma_i I_{xi} + \sum J_{ij} I_{xi} I_{xj}) T)\}_{kk-ll}}{(-\sum \sigma_i I_{xi} + \sum J_{ij} I_{xi} I_{xj})_{kk-ll}}, \quad [15a]$$

$$B_{kl} = (\sum J_{ij} (I_{zi} I_{zj} + I_{yi} I_{yj}))_{kl} \frac{\{\exp(-i(\sum \sigma_i I_{xi} + \sum J_{ij} I_{xi} I_{xj}) T)\}_{kk-ll}}{(\sum \sigma_i I_{xi} + \sum J_{ij} I_{xi} I_{xj})_{kk-ll}}. \quad [15b]$$

( $M_{kk-ll}$  is short for  $M_{kk} - M_{ll}$ .)

Since  $\|\mathcal{H}_{cs} T\| \gg 1$ ,  $\|A\| \sim \|B\| \sim \|\mathcal{H}_J\|/\|\mathcal{H}_{cs}\| \ll 1$  if the system is first order, and therefore  $U$  is close to 1. Since this sequence is cyclic, the usual ansatz  $U = \exp(-i\mathcal{H}(2T))$  can be made, and then  $\|\mathcal{H}(2T)\| \ll 1$ . Thus this sequence may produce a usable  $\mathcal{H}_0$ , but the poor convergence means that this argument is not rigorous.

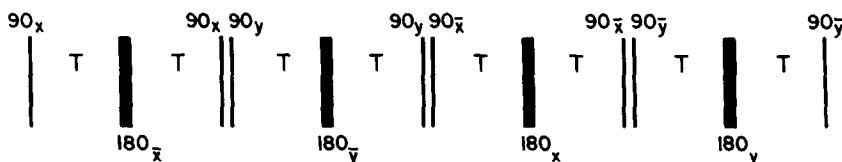


FIG. 14. A simple pulse sequence for  $4k$ -quantum selection in isotropic systems. The sequence for  $\mathcal{H}_0$  is  $90_x - T - 180_{\bar{x}} - T - 90_{\bar{x}}$ ; the echo pulse causes partial refocusing of the chemical shifts.

Figure 15 shows the selectivity of a first-order  $4k$ -quantum selective sequence as a function of  $T$ ; the molecular parameters correspond to methanol at 270 MHz (21). The selectivity is expected to be an extremely complicated function, because  $\bar{\mathcal{H}}$  changes as  $T$  changes. Still, there is a region where the selectivity is good and  $\|\mathcal{H}_0\|$  is small; if  $T$  is chosen from this region, the first-order sequence can be repeated several times to give a large signal, as shown in Fig. 16. For example, one sequence which will produce a large four-quantum signal is 3 cycles of first-order selection with  $T = 12.0$  ms. The total duration of the sequence is 576 ms, which is short enough to neglect relaxation effects (as is implicitly done in all of these computer calculations). Higher-order selectivity is of course possible in isotropic systems as well, when relaxation times are long enough to allow many subcycles. It should be noted, however, that isotropic selective sequences are not as easy to design as anisotropic ones, and that relaxation times provide a serious constraint for protons. The  $J$  couplings are larger with other nuclei (for example,  $^{13}\text{C}$  and  $^{19}\text{F}$ ) and therefore selectivity is simpler in those systems.

#### CONCLUSIONS

Computer calculations have been presented which verify the average Hamiltonian theory calculation of earlier work. The selectivity and signal intensity have the form

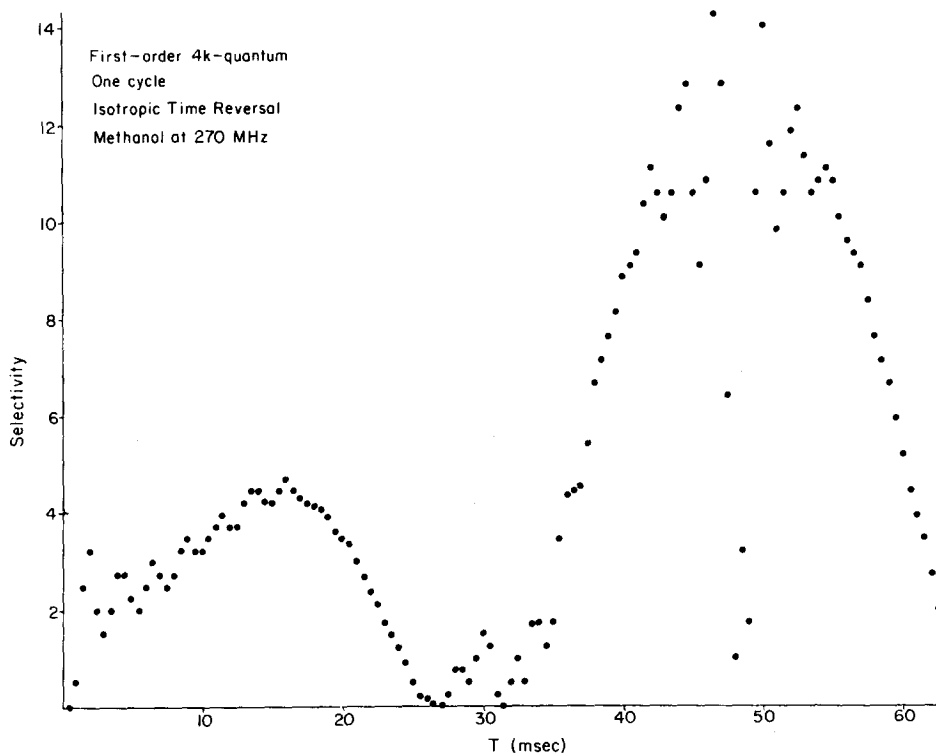


FIG. 15. The coherence selectivity of a first-order  $4k$ -quantum selective sequence for isotropic methanol at 270 MHz. The pulse sequence is a symmetrized version of Fig. 14.

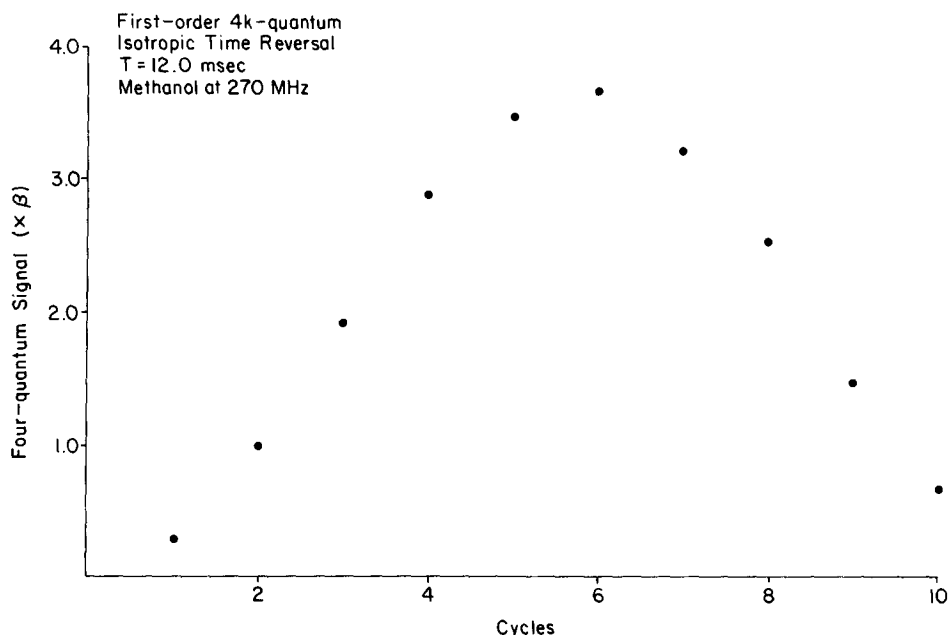


FIG. 16. The signal produced by fixing  $T$  at 12.0 ms and incrementing the number of cycles, for 4k-quantum selection on methanol at 270 MHz.

expected from those calculations. In addition, these calculations show that the region of convergence of the Magnus expansion agrees with earlier estimates, and that the selectivity is still good near the limits of convergence. Simplified pulse sequences for isotropic and anisotropic systems have been shown to provide signal enhancements. Since these computer calculations are exact (to the extent that the spins follow the density matrix equation of motion in the absence of relaxation) it may be concluded that selective sequences provide a practical technique for signal enhancement.

#### ACKNOWLEDGMENTS

As with our previous paper, we are most grateful for help from Dr. Melvin Klein and Dr. K. Wiley of the Laboratory of Chemical Biodynamics, Lawrence Berkeley Laboratory, and from other members of the Pines group. W.S.W. held a National Science Foundation Graduate Fellowship. This work was supported by the Director, Office of Energy Research, Office of Basic Energy Sciences, Materials Sciences Division of the U.S. Department of Energy under Contract DE-AC03-76SF00098.

#### REFERENCES

1. J. B. MURDOCH, W. S. WARREN, D. P. WEITEKAMP, AND A. PINES, *J. Magn. Reson.* **60**, 205 (1984).
2. S. HSI, H. ZIMMERMANN, AND Z. LUZ, *J. Chem. Phys.* **69**, 4126 (1978).
3. J. TANG AND A. PINES, *J. Chem. Phys.* **73**, 2512 (1980).
4. S. SINTON AND A. PINES, *Chem. Phys. Lett.* **76**, 263 (1980).
5. A. WOKAUN AND R. R. ERNST, *Mol. Phys.* **36**, 317 (1978).
6. M. E. STOLL, A. J. VEGA, AND R. W. VAUGHAN, *J. Chem. Phys.* **67**, 2029 (1977).
7. R. POUPKO, R. L. VOLD, AND R. R. VOLD, *J. Magn. Reson.* **34**, 67 (1979).

8. G. BODENHAUSEN, R. L. VOLD, AND R. R. VOLD, *J. Magn. Reson.* **37**, 93 (1980).
9. J. TANG AND A. PINES, *J. Chem. Phys.* **72**, 3290 (1980).
10. S. EMID, A. BAX, J. KONIJNENDIJK, J. SMIDT, AND A. PINES, *Physica B* **96**, 333 (1979).
11. W. S. WARREN AND A. PINES, *J. Am. Chem. Soc.* **103**, 1613 (1981).
12. W. S. WARREN AND A. PINES, *J. Chem. Phys.* **74**, 2808 (1981); G. DROBNY, A. PINES, S. SINTON, W. S. WARREN, AND D. P. WEITEKAMP, *Phil. Trans. Roy. Soc. London Ser. A* **299**, 585 (1981).
13. W. S. WARREN, S. SINTON, D. P. WEITEKAMP, AND A. PINES, *Phys. Rev. Lett.* **43**, 1791 (1979).
14. W. S. WARREN, D. P. WEITEKAMP, AND A. PINES, *J. Magn. Reson.* **40**, 581 (1980).
15. W. S. WARREN, D. P. WEITEKAMP, AND A. PINES, *J. Chem. Phys.* **73**, 2084 (1980).
16. J. S. WAUGH, L. M. HUBER, AND U. HAEBERLEN, *Phys. Rev. Lett.* **20**, 180 (1968).
17. U. HAEBERLEN, "High Resolution NMR in Solids: Selective Averaging," Academic Press, New York, 1976.
18. P. L. CORIO, "Structure of High-Resolution NMR Spectra," Appendix III, Academic Press, New York, 1966.
19. H. Y. CARR AND E. M. PURCELL, *Phys. Rev.* **94**, 630 (1954); S. MEIBOOM AND G. GILL, *Rev. Sci. Instrum.* **29**, 688 (1958).
20. W.-K. RHIM, A. PINES, AND J. S. WAUGH, *Phys. Rev. B* **3**, 684 (1971).
21. W. S. WARREN AND A. PINES, *Chem. Phys. Lett.* **88**, 441 (1982).